analytical chemistry

Technical Note

pubs.acs.org/ac

Molecular Logic Gates on DNA Origami Nanostructures for MicroRNA Diagnostics

Dongfang Wang,[†] Yanming Fu,[†] Juan Yan,[†,‡] Bin Zhao,[†] Bin Dai,[†] Jie Chao,[†] Huajie Liu,[†] Dannong He,[‡] Yi Zhang,[†] Chunhai Fan,[†] and Shiping Song*[,†]

[†]Laboratory of Physical Biology, Shanghai Institute of Applied Physics, Chinese Academy of Sciences, Shanghai 201800, China

[‡]National Engineering Research Center for Nanotechnology, Shanghai 200241, China

Supporting Information

ABSTRACT: Molecular computing holds great promise for diagnosis and treatment of diseases at the molecular level; nevertheless, designing molecular logic gates to operate programmably and autonomously for molecular diagnostics still remains challenging. We designed logic gates on DNA Origami for microRNA analysis. As a demonstration, two indicators of heart failure, microRNA-21 and microRNA-195, were selected as the logic inputs. The logic gates contain two main modules: computation module and output module, performing in a single DNA Origami nanostructure. The computation module recognizes disease indicators, while the output module display different nanoscale symbols, "+" (positive) or "−" (negative), depending on the computing results. We demonstrated that the molecular logic gates worked well with single and two input combinations.

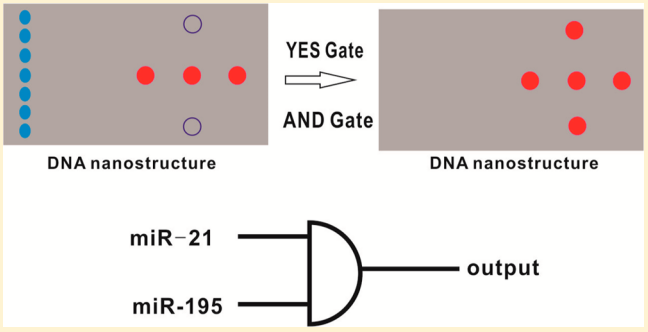

Since the first experiment demonstration of carrying out computations at the molecular level,[1] early biomolecular computer research had been focused on molecule-based computation for complex computational problems.[1−3] Later, people realized that biomolecular computers to interact with naturally biomolecules are much more important than their computational power.[4] Molecular computers,[5−7] which used biological molecules as inputs and outputs, were capable of controlling biological progress such as gene regulation,[8,9] disease diagnostics,[10] and biomarker detection.[4,11] For example, Shapiro[8] designed a molecular computer that can autonomously make decisions when to release a drug for a disease or a drug suppressor, depending on the positive or negative diagnosis. Thus, diagnosis of diseases at the molecular level paves the way to disease treatment in vivo intelligently. Molecular logic gates hold great promise for molecular diagnostics that have become more and more important to genetic disease, human cancers, and infectious diseases. In this work, we integrate the DNA Origami with logic capability for molecular diagnostics and demonstrate its availability in principle.

DNA Origami is designed with single strand viral DNA and more than two hundred short staple DNA strands.[12] The surfaces of DNA Origami are fully addressable, allowing for the incorporation of multiple ligands,[13] oligonucleotides, antibodies,[14] hormones, labels for biosensor,[15] and so forth. They might be used for efficient and site-specific drug delivery and release.[14,16] The potentials of DNA Origami have attracted much attention in various areas, including nanophotonics[17] and biomedical studies. Here we designed logic gates on DNA Origami and intend to diagnose a disease by analyzing two disease indicators. Previous clinical studies demonstrated that one type of disease is often associated with more than one gene indicators and their logical relationship often indicates different states of the disease.[18] MicroRNA expression data, especially, in various diseases demonstrates that disease cells have different microRNA profiles compared with normal cells, thus underscoring the tremendous diagnostic potential of microRNAs in diseases such as cancer and heart disease.[19−21] As a demonstration, we select two indicators of heart failure, microRNA-21 (miR-21)[22] and microRNA-195 (miR-195),[23] as the logic inputs. Our logic gates contain two main modules: computation module and output module. The computation module receives and analyzes disease indicators, while the output module displays different symbols, depending on the computing results. The two modules connect by a signal DNA, which transfers information from the computation module to the output module. Output symbols on DNA Origami can be visually observed by atomic force microscopy (AFM).

EXPERIMENTAL SECTION

Materials. All stable DNA strands were purchased from Generay Inc. (Shanghai, P. R. China), and each strand was normalized to 100 μM. MicroRNA-21 and microRNA-195

Received: November 12, 2013
Accepted: January 21, 2014
Published: January 21, 2014

Scheme 1. DNA Origami-based logic gates[a]

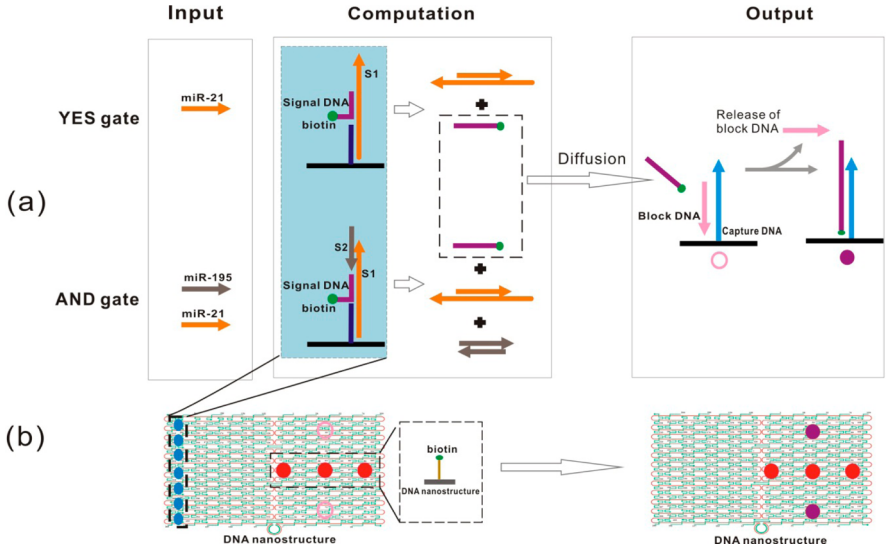

[a](a) Logic gates contain two modules: computation module and output module. The computation module receives and analyzes disease indicator inputs (microRNA), while the output module displays different symbols ("−" or "+"), depending on the computing results. The two modules are connected by a biotinylated signal DNA, which transfers information from the computation module to the output module. The YES gate allows only one input, while the AND gate accepts two inputs. STV is added to bind to biotinylated DNA after the logic computation, and the computational results can be visually observed by AFM. (b) Schematic illustration of AFM images of logic results.

were purchased from Invitrogen Inc. Synthetic ribonucleotides were used to obtain mature miRNAs. Microcon Centrifugal Filter Devices (100000 MWCO, catalog no. 42413) were purchased from Millipore. M13 viral DNA were purchased from New England Biolabs, Inc. (NEB, catalog no. N4040S), and STV was from AMRESCO Inc. (catalog no: E497).

DNA Origami Assembly and Hybridization. Rectangular-shaped DNA Origami tiles were formed according to Rothemud's method.[12] M13mp18 DNA was mixed with over 200 short DNA strands with a molar ratio of 1:5 (5 nM M13mp18 DNA, 25 nM each stable DNA) in 1 × tris-acetate-ethyenediaminetetraacetic acid (TAE)/Mg^{2+} buffer (Tris, 40 mM; acetic acid, 20 mM; EDTA, 2 mM; and magnesium acetate, 12.5 mM; pH 8.0). Block DNA (final concentration: 200 nM) were then added before annealing. Then the mixture was annealed in a polymerase chain reaction (PCR) machine at the temperature ranging from 95 to 19 °C at a rate of 0.1 °C every 10 s. After annealing, YES gate DNA or AND gate DNA (500 nM) were added for hybridization with gate helpers on Origami at 35 °C for 30 min. Then the mixture was purified using Microcon centrifugal filter devices (100000 MWCO, 3000*g* speed, 10 min, 4 times) followed by washing with 1 × TAE/Mg^{2+}, and about 40 μL 2.5 nM DNA Origami was collected.

AFM Imaging. A final concentration of 100 nM microRNA21 or microRNA195 was added to DNA Origami (2.5 nM, 10 μL) at 30 °C for 6 h. Then, 100 nM streptavidin was added for 30 min at 37 °C. Three microliters of samples were deposited onto freshly cleaved mica for 3 min for adsorption. Thirty microliters of 1 × TAE/Mg^{2+} buffer was added to the liquid cell, and the sample was scanned in a tapping mode on a commercial AFM (Multimode 8, Bruker Inc.) with silicon nitride cantilevers (NP-S, Bruker Inc.)

Native Polyacrylamide Gel Electrophoresis (PAGE). The DNA solution mixed with 6× loading buffer (TEK buffer, pH 8.0, 50% glycerol, 0.25% bromphenol blue) was analyzed in 8% native polyacrylamide gel. The electrophoresis was conducted in 1 × TAE (Mg^{2+} concentration: 12.5 mM; pH8.0) at a constant voltage of 90 V for 1.5 h. The gels were scanned by a UV transilluminator after staining with Gel Red.

RESULTS AND DISCUSSION

Our system is designed to determine whether only miR-21 or both miR-21 and miR-195 are present in a sample. A schematic illustration of logic gates on DNA Origami is shown in Scheme 1. The miR-195 and miR-21 are designed as inputs of logic gates, and "+" or "−" as the logic outputs, indicating positive diagnostics or negative diagnostics, respectively. In order to visually observe the output symbols, a protein label, streptavidin (STV), which has a high affinity binding constant toward biotin, is selected as the contrast label for AFM imaging.[24−26] Computation module is implemented by Gate DNA. YES Gate DNA consists of S1 and signal DNA (Scheme 1a, YES Gate), and AND gate DNA consists of S1, S2, and signal DNA (Scheme 1a, AND Gate). Signal DNA will release from Gate DNA and become free in the solution when it receives the correct target inputs. To increase the concentration of free signal DNA in solution, we used 7 staple DNA that would hybridize with the gate DNA. Theoretically, the more signal DNA release from DNA Origami, the more likely the capture DNA will hybridize with it. The output module consists of three biotinylated DNA strands and two capture DNA. The capture DNA is blocked by the block DNA by default so that it will not hybridize with the gate DNA. In the 3′ end of the capture DNA, there are 5 base toeholds through which the free signal DNA can displace the block DNA and hybridize with capture DNA. Three biotinylated staples are used as negative output "−" after they are combined with STV, while positive output "+" can only be obtained when the captured DNA hybridize with the free biotinylated signal DNA (Scheme 1b). After the input of analysts, signal DNA would release from the DNA Origami and diffuse into solution. The free biotinylated signal DNA then hybridize with capture DNA by displacing the

dx.doi.org/10.1021/ac403661z | *Anal. Chem.* 2014, 86, 1932−1936

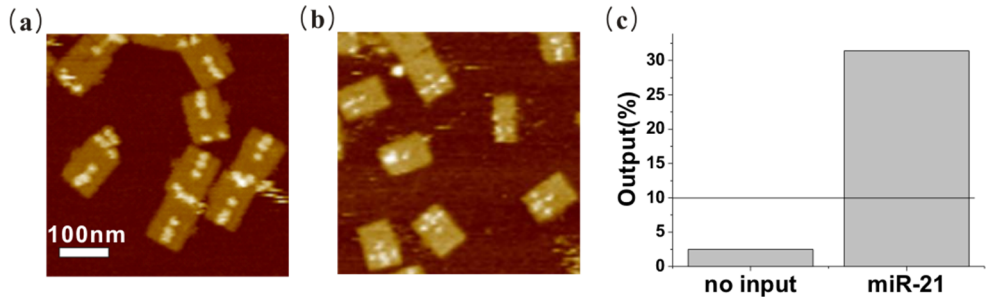

Figure 1. AFM images of YES gate. (a) No input. (b) 100 nM miR-21 input. Scale bar: 100 nm. (c) YES gate output efficiency. The outputs resulted from three replicates for each experiment. The threshold is set as 10%.

block DNA. STV is then added to bind to biotin, and logic outputs could be observed by AFM. This system can be described as a simple functional model of YES and AND logic gates. We first tried the YES gate. YES gate can be interpreted as "turn-on" model of single analyst diagnosis. The output signal is obtained when the single input is presented. DNA Origami was first prepared with block DNA added, then YES gate DNA was added to hybridize with gate strands on Origami. Figure 1a demonstrated the gate DNA was hybridized with gate strands successfully (see Figure s1 of the Supporting Information for more details). After removing extra helpers and free gate DNA by centrifugation, the YES gate was ready for miR-21 detection. After input of miR-21, it would displace the signal DNA by toehold-mediated strand displacement. The free biotinylated signal DNA would then hybridize with capture DNA by displacing the block DNA. Figure 1b shows the signal DNA was displaced and "+" appeared on the DNA Origami (see Figure s2 of the Supporting Information for more details). Similarly, the detection of miR-195 can also be achieved by designing such a YES gate. Figure 1c shows the logic output efficiency of the YES gate. The experimental results were reproduced at least three times to ensure the reliability of the results. RSD for no input and miR-21 are about 0.93% and 3.5%. We then tested the AND logic gate in this system. AND logic is represented by the situation where the output of the gate occurs only when both inputs are present. The AND logic gate presented here queries two microRNAs to determine whether both of them are present. The AND gate in our system differs with the YES gate only when the gate DNA consists of S1, S2, and signal DNA. That is, only the input of both miR-21 and miR-195 can release the signal DNA. Experiments were performed by testing the AND gate with all possible input combinations of miR-21 and miR-195. Figure 2 shows the different output results and efficiency of AND gates. In the case of no input (Figure 2a) or only single input miR-195 (Figure 2b) or miR-21 (Figure 2c), the signal DNA remained on the DNA Origami and only "−" could be observed in the output region (see Figures s3−s5 of the Supporting Information for more details). In the case of both inputs (Figure 2d), positive output "+" appears on the DNA Origami (see Figure s6 of the Supporting Information for more details). Figure 2e shows the logic output efficiency of the AND gate. To test the specificity of the system, three miR-21 analogues containing mismatched nucleotides and a noncognatic DNA were designed. As seen in Figures s7−s10 of the Supporting Information, no significant discrepancy is observed compared with the blank control (Figure s1 of the Supporting Information), demonstrating the high selectivity of the logic gates.

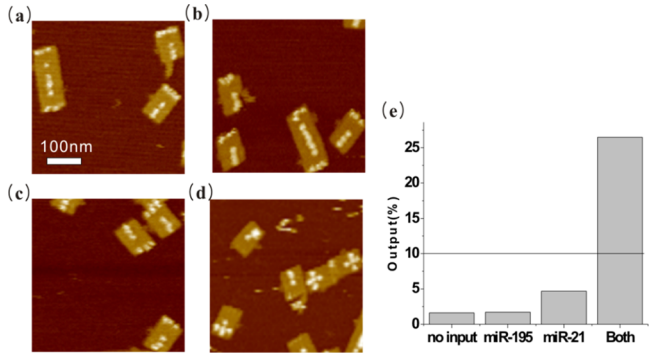

Figure 2. AFM images of the AND gate. (a) No input, (b) only miR-195 input, (c) only miR-21 input, and (d) 100 nM miR-21 and 100 nM miR-195 input. Scale bar: 100 nm. (e) The AND gate output efficiency. The outputs resulted from three replicates for each experiment. The threshold is set as 10%.

The YES and AND logic gates were further confirmed by native polyacrylamide gel electrophoresis (PAGE). In Figure 3, the DNAs contained in different bands have been determined. We first identify the computation of YES and AND logic gates, which receive the input signals and release the signal DNA. In the YES logic gate, with the input of miR-21, lane 4 in Figure 3a contains the S1 and miR-21 complex, miR-21, and the output product signal DNA. Without the input of miR-21, the lane 3 only contains the S1 and signal DNA complex, which indicate the signal DNA was not released. In the AND logic gate, lane 8 contains the S1 and miR-21 complex, miR-21, miR195, and S2 complex, and the output product signal DNA. For either no input or just one signal inputs (miR-21 or miR-195), as seen in lanes 5−7 in the Figure 3a, no signal DNA is observed, demonstrating the viability of YES and AND logic gates. The strand displacement of the reporter DNA by the signal DNA is also investigated in Figure 3b. In the lane 3, after the addition of the signal DNA, the main band moves slower, which means the block DNA is released from the signal DNA and the formed product is the doubled strand of the signal DNA and the capture DNA. Thus, this is a reliable molecular device that functions as designed.

Presently, most of investigators suffer from the problem of low yield. In this work, the positive output efficiency of the logic gates is about 26%~32% in our system (Table 1). The relatively low yield may arise from several factors: (1) the signal DNA may be not completely released through toehold-mediated displacement from the gate DNA after the analysts input and (2) the negative charged DNA Origami may hinder the close proximity of free signal DNA in the solution due to electrostatic repulsion. It is important to note that the signal

dx.doi.org/10.1021/ac403661z | Anal. Chem. 2014, 86, 1932−1936

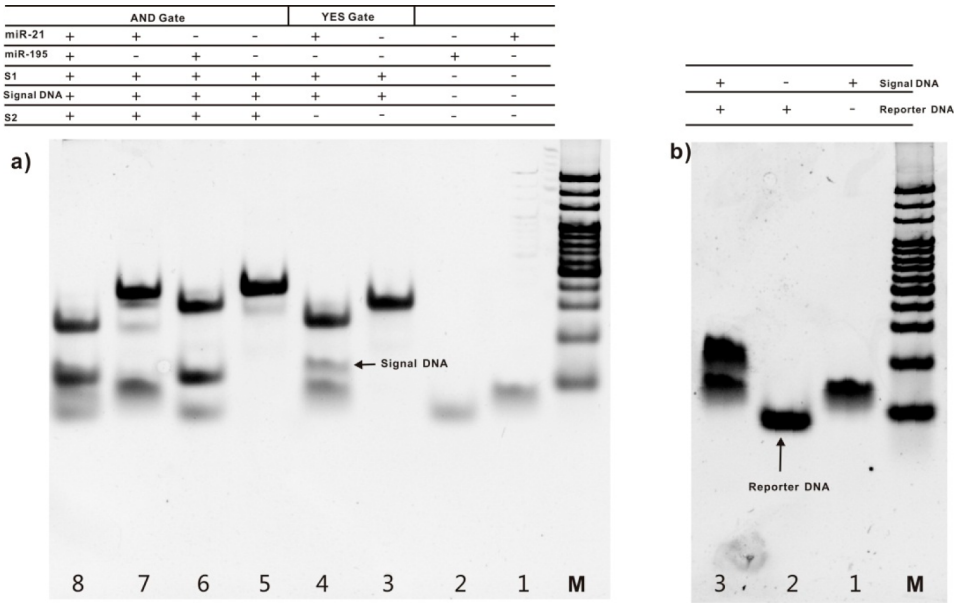

Figure 3. Native 8% polyacrylamide gel analysis of the logic gates. DNA strands added in every lane are indicated in the table. (a) Gel analysis of YES and AND logic gates. Both outputs of the logic gates are the signal DNA. Concentrations for each DNA in PAGE are all 0.5 μM. Lane M: 20 bp DNA marker. (b) Gel analysis of DNA displacement of reporter DNA by the signal DNA. Concentrations for reporter DNA and signal DNA are 0.5 and 1 μM, respectively.

Table 1. Statistical Analysis for YES Gate and AND Gate on the DNA Origami[a]

	input	output ("+")	Origami no.	efficiency (%)
YES gate	no input	2.5	102	2.5
	miR-21	22	79	31.4
	mismatch-1	2	99	2.0
	mismatch-2	3.5	83	4.2
	mismatch-3	2	82	2.4
	noncognatic RNA	1	75	1.3
AND gate	no input	0.5	32	1.6
	miR-195	1.5	88	1.7
	miR-21	4.5	96	4.7
	miR-21 and miR-195	13	49	26.5

[a]Note: completed "+" is defined as 1 and uncompleted "+" is defined as 0.5. Output "−" is defined as 0.

transduction used in this system has deep implication not only in the logic computing but also in the construction of more complex logic circuits in the DNA Origami chip. Although the output in the system is quite clear (positive/negative: ~10) and reproducible, there is still much to do to improve the system. While DNA walker[27,28] has been used to transfer cargos and build assembly lines on the DNA Origami,[29] it may also be an alternative way of signal transduction in the logic computing.

CONCLUSION

In summary, we have demonstrated DNA Origami-based logic gates for microRNA diagnostics. The logic gates can perform simple computing and display correct symbols in response to disease indicators. The system also demonstrates a "lab on DNA Origami" prototype, which could be applied to develop DNA Origami-based computing for disease diagnostics and therapeutics. On the basis of the prototype, fluorescence and electrochemistry signals might be candidates instead of AFM symbols to achieve the readout of the logic gates. Further, the system has potential to logically analyze the biological microenvironment and activate or administer the requisite drug upon positive diagnosis of a disease, which is an acknowledged challenge for molecular computing to operate programmably and autonomously to fight disease, based on the molecular composition of the microenvironment.

ASSOCIATED CONTENT

Supporting Information

Ten supporting figures, 6 DNA and microRNA sequences, and 226 DNA Origami sequences. This material is available free of charge via the Internet at http://pubs.acs.org.

AUTHOR INFORMATION

Corresponding Author

*E-mail: spsong@sinap.ac.cn.

Notes

The authors declare no competing financial interest.

ACKNOWLEDGMENTS

We thank the National Basic Research Program of China (973 program, No. 2013CB932802 and 2012CB932600) and the National Science Foundation of China (91127037, 91123037, and 21373260) for financial support.

REFERENCES

(1) Adleman, L. *Science* **1994**, *266*, 1021−1024.
(2) Lipton, R. J. *Science* **1995**, *268*, 542−545.
(3) Ouyang, Q.; Kaplan, P. D.; Liu, S.; Libchaber, A. *Science* **1997**, *278*, 446−449.
(4) Gil, B.; Kahan-Hanum, M.; Skirtenko, N.; Adar, R.; Shapiro, E. *Nano Lett.* **2011**, *11*, 2989−2996.
(5) Chen, J.; Wood, D. H. *Proc. Natl. Acad. Sci. U.S.A.* **2000**, *97*, 1328−1330.
(6) Benenson, Y.; Paz-Elizur, T.; Adar, R.; Keinan, E.; Livneh, Z.; Shapiro, E. *Nature* **2001**, *414*, 430−434.

(7) Adar, R.; Benenson, Y.; Linshiz, G.; Rosner, A.; Tishby, N.; Shapiro, E. *Proc. Natl. Acad. Sci. U.S.A.* **2004**, *101*, 9960−9965.
(8) Benenson, Y.; Gil, B.; Ben-Dor, U.; Adar, R.; Shapiro, E. *Nature* **2004**, *429*, 423−429.
(9) Rinaudo, K.; Bleris, L.; Maddamsetti, R.; Subramanian, S.; Weiss, R.; Benenson, Y. *Nat. Biotechnol.* **2007**, *25*, 795−801.
(10) Konry, T.; Walt, D. R. *J. Am. Chem. Soc.* **2009**, *131*, 13232−13233.
(11) Hemphill, J.; Deiters, A. *J. Am. Chem. Soc.* **2013**, *135*, 10512−10518.
(12) Rothemund, P. W. K. *Nature* **2006**, *440*, 297−302.
(13) Fu, Y.; Zeng, D.; Chao, J.; Jin, Y.; Zhang, Z.; Liu, H.; Li, D.; Ma, H.; Huang, Q.; Gothelf, K. V.; Fan, C. *J. Am. Chem. Soc.* **2013**, *135*, 696−702.
(14) Douglas, S. M.; Bachelet, I.; Church, G. M. *Science* **2012**, *335*, 831−834.
(15) Ke, Y.; Lindsay, S.; Chang, Y.; Liu, Y.; Yan, H. *Science* **2008**, *319*, 180−183.
(16) Pinheiro, A. V.; Han, D.; Shih, W. M.; Yan, H. *Nat. Nano.* **2011**, *6*, 763−772.
(17) Kuzyk, A.; Schreiber, R.; Fan, Z.; Pardatscher, G.; Roller, E.-M.; Hogele, A.; Simmel, F. C.; Govorov, A. O.; Liedl, T. *Nature* **2012**, *483*, 311−314.
(18) Shen, J.; Stass, S. A.; Jiang, F. *Cancer Lett.* **2013**, *329*, 125−136.
(19) Bartel, D. P. *Cell* **2004**, *116*, 281−297.
(20) Bentwich, I.; Avniel, A.; Karov, Y.; Aharonov, R.; Gilad, S.; Barad, O.; Barzilai, A.; Einat, P.; Einav, U.; Meiri, E.; Sharon, E.; Spector, Y.; Bentwich, Z. *Nat. Genet.* **2005**, *37*, 766−770.
(21) Berezikov, E.; Guryev, V.; van de Belt, J.; Wienholds, E.; Plasterk, R. H. A.; Cuppen, E. *Cell* **2005**, *120*, 21−24.
(22) Thum, T.; Galuppo, P.; Wolf, C.; Fiedler, J.; Kneitz, S.; van Laake, L. W.; Doevendans, P. A.; Mummery, C. L.; Borlak, J.; Haverich, A.; Gross, C.; Engelhardt, S.; Ertl, G.; Bauersachs, J. *Circulation* **2007**, *116*, 258−267.
(23) van Rooij, E.; Sutherland, L. B.; Liu, N.; Williams, A. H.; McAnally, J.; Gerard, R. D.; Richardson, J. A.; Olson, E. N. *Proc. Natl. Acad. Sci. U.S.A.* **2006**, *103*, 18255−18260.
(24) Zhang, Z.; Wang, Y.; Fan, C.; Li, C.; Li, Y.; Qian, L.; Fu, Y.; Shi, Y.; Hu, J.; He, L. *Adv. Mater.* **2010**, *9999*, 2672−2675.
(25) Wong, N. Y.; Xing, H.; Tan, L. H.; Lu, Y. *J. Am. Chem. Soc.* **2013**, *135*, 2931−2934.
(26) Sharma, J.; Ke, Y.; Lin, C.; Chhabra, R.; Wang, Q.; Nangreave, J.; Liu, Y.; Yan, H. *Angew. Chem., Int. Ed.* **2008**, *47*, 5157−5159.
(27) Wickham, S. F. J.; Bath, J.; Katsuda, Y.; Endo, M.; Hidaka, K.; Sugiyama, H.; Turberfield, A. J. *Nat. Nano.* **2012**, *7*, 169−173.
(28) Wickham, S. F. J.; Endo, M.; Katsuda, Y.; Hidaka, K.; Bath, J.; Sugiyama, H.; Turberfield, A. J. *Nat. Nano.* **2011**, *6*, 166−169.
(29) Gu, H.; Chao, J.; Xiao, S.-J.; Seeman, N. C. *Nature* **2010**, *465*, 202−205.